JOURNAL OF CATALYSIS **164,** 301–314 (1996)
ARTICLE NO. 0386

Solid-State ^{13}C MAS NMR Study of Methanol-to-Hydrocarbon Chemistry over H-SAPO-34

Fathollah Salehirad and Michael W. Anderson

Department of Chemistry, UMIST, P.O. Box 88, Manchester M60 1QD, UK

Received September 11, 1995; revised July 10, 1996; accepted August 9, 1996

^{13}C solid-state MAS NMR was used to probe the chemistry of a number of species involved in the methanol-to-hydrocarbon process over H-SAPO-34 molecular sieve at both high (573 K) and low (473–563 K) temperature ranges and at very low conversion ($<$0.1%). Isobutane was the only hydrocarbon product observed at 473 and 573 K. Evidence for the operation of a stepwise methylation reaction via surface-bound species derives from, first, the treatment of several samples with different loadings of methanol at 523–563 K and, second, when either [^{13}C]methanol is coadsorbed with [^{12}C]ethene over the catalyst or [^{12}C]ethene is reacted with pre-[^{13}C]methylated SAPO-34. The hydrocarbon products in these experiments were mainly isobutane and isopentane as well as methane, ethene, and propane. Based on these experimental findings, a number of mechanistic approaches concerning the very first stages of the reaction are discussed.

INTRODUCTION

Methanol conversion over microporous molecular sieves such as zeolites and zeotype materials is a remarkable reaction which has been extensively studied in recent years (1 –10). One objective of this considerable research effort has been to attempt to elucidate the mechanism of formation of the initial products containing C−C bonds. Some of these products can be observed at reaction temperatures as low as 473–563 K (3), although industrial temperatures for this conversion are normally in the range of 623–753 K (11). A variety of techniques such as *in situ* Fourier transform infrared (12–14) (FT-IR), flow reactor/gas chromatography–mass spectrometry (3, 4, 15, 16) (GC-MS), temperature programmed desorption (14, 17, 18) (TPD), differential scanning calorimetry (19, 20) (DSC), and *in situ* solid-state ^{13}C magic-angle spinning nuclear magnetic resonance (8, 21–26) (MAS NMR) have been used in these studies. However, the complexity of reaction due to rapid secondary reactions as well as limitations of available techniques for monitoring this process have always been an obstruction for chemists in providing conclusive evidence for the mechanism. To date a number of mechanistic approaches have been proposed for this conversion process mainly over H-ZSM-5; however, only two, namely carbene (1, 27) and dimethyl oxonium methylide (28–30) proposals, have received significant experimental support. The common feature of both approaches, which is the involvement of the zeolite conjugate base which acts as a base toward a nonbonded reactant species, has been questioned (31). A mechanism based on the intermediacy of surface-bound species (methoxy groups), which have been observed spectroscopically (12, 13, 32–35), has been proposed for methanol conversion over H-ZSM-5 by Hutchings *et al.* (31). They concluded that the surface bound species is deprotonated via a nearby zeolite basic site (“adjacent Al–O site”) to a surface bound carbene which in turn engages in C−C bond formation. It is also reported (36) that methane and ethene are primary products since large amounts have been observed as the reactivity of the methylating agent was reduced. Here we report on the use of ^{13}C MAS NMR to follow the course of methanol conversion over H-SAPO-34 using sealed capsules containing the catalyst with different loadings of ^{13}C enriched methanol. Being isostructural with the natural zeolite chabazite, SAPO-34 molecular sieve has a cage structure rather than a channel structure as in ZSM-5. H-SAPO-34 also has lower acidity (37–38) than that of H-ZSM-5. These two features have consequences (especially the former) with respect to the catalytic performance of the molecular sieve (38) such that the catalyst is selective for synthesis of light olefins, i.e., C_2–C_4 hydrocarbons. The lower acidity and high selectivity of H-SAPO-34 in contrast to H-ZSM-5 enable a better understanding of the conversion reaction mechanism using ^{13}C solid-state NMR.

EXPERIMENTAL

Preparation

SAPO-34 was prepared based on the method described in the original patent (39) from a gel of composition $Al_2O_3 : P_2O_5 : 0.3SiO_2 : (TEA)_2O : 50H_2O$. The sources of these elements were aluminum isopropoxide, 85% phosphoric acid, tetraethylammonium hydroxide as templating agent and aqueous solution of 30% SiO_2. The product was determined by X-ray Diffraction to be phase-pure SAPO-34 molecular sieve. Calcination was carried out at

0021-9517/96 $18.00

823 K for 10 h to remove the organic template prior to catalytic testing. ^{29}Si, ^{31}P, and ^{27}Al NMR of the calcined sample also showed it to be a pure SAPO phase with a very small amount of octahedral aluminum.

Catalysis and MAS NMR Spectroscopy

Methanol (MeOH) 99% enriched in ^{13}C (MSD ISOTOPES) was purified by the freeze–pump–thaw method. Catalysts (typically 50 mg) for ^{13}C MAS NMR were placed in specially designed pyrex microreactors (26), in which they were activated under vacuum (ca. 10^{-4} mb) at 673 K overnight. They were loaded with MeOH (0.5, 1, and 3 molecules/acid site) and ethene (BOC) (0.5, 1, and 1.89 molecules/acid site) and sealed under liquid nitrogen. These capsules were heated at various reaction temperatures for a period of 2.5 min (in the case of prolonged) heating the time is indicated on the spectra). All ^{13}C proton decoupled {H} MAS, ^{1}H MAS, and ^{2}H static NMR spectra were recorded at ambient temperature on a Bruker MSL 400 (61.42 MHz for D, 100.613 MHz for ^{13}C, and 400.13 MHz for ^{1}H) spectrometer using Chemagnetics APEX 400 pencil, 4 mm, 7 mm, and static probes. High-power decoupling experiments were carried out with 45° ^{13}C pulse and 5 s repetition time which were found to be adequate to yield quantitatively reliable spectra. ^{1}H MAS NMR spectrum was recorded using the Hahn-echo pulse sequence (40) to eliminate background signals from outside the coil. The sample for this experiment was prepared by reaction of CH_3OH over H-SAPO-34 (1 : 1 reactant molecule per acid site) at 473 K for 15 min followed by pumping the sample for one more hour at the same temperature under high vacuum. The sealed sample was then transferred into a glove box and purged four times with dry, pure Ar to ensure that no water vapor was introduced. Subsequently it was transferred into an air-tight 4-mm Bruker rotor and immediately capped. D-Methylated catalyst for static deuterium NMR was prepared by reaction of CD_3OH over H-SAPO-34 (1 : 1) under the same conditions mentioned above and finally sealed in a 9-mm (i.d.) glass ampoule under liquid N_2 while attached to a vacuum line. The ^{2}H static spectrum was obtained using the composite multiple pulse sequence described by Siminovitch *et al.* (41). This permits even excitation of very broad NMR resonances allowing static powder patterns even up to 180,000 Hz to be observed. Both $^{13}CH_3OH$ (0.5 : 1) and $^{12}C_2H_4$ (0.5 : 1) were coadsorbed, respectively, over a measured amount of the dehydrated catalyst via a gas-handling vacuum line followed by sealing at liquid N_2 temperature in order to examine the effect of ethene on methanol conversion. A similar sample was also prepared with the adsorption of $^{12}C_2H_4$ (1 : 1) onto the pre-[^{13}C]methylated catalyst in the same vacuum line at room temperature when the first step, i.e., methylation of H-SAPO-34 as mentioned above, was completed. ^{13}C CPMAS NMR spectra were performed with 2 ms contact time and 5 min recycle time. Magic-angle spinning (2.7–5 kHz for ^{13}C and 10 kHz for ^{1}H) was used in all experiments. Depending on product concentration 200–15000 transients were performed in this study.

Catalysis and Gas Chromatography (GC)

Catalytic tests were performed in a flow reactor at temperatures of 623 and 673 K using two separate reactants (MeOH and ethene). Catalyst pellets (40/60 mesh) or powder (0.1 g) were used with ethene (weight hourly space velocity WHSV = 0.7 and 10.48 h^{-1}) and methanol (WHSV = 6 h^{-1}). In the case of ethene, products were analyzed using a gas chromatograph (Varian 3600) with a DB-1 fused silica capillary column (60 m × 0.32 mm i.d.) and flame ionization detector. In the methanol conversion the spent catalyst was packed into a 7-mm zirconia MAS rotor under argon gas after the GC experiment for 5 min time on stream (TOS). Argon was also used as a carrier gas (38 ml/min) for the flow reaction system to convey reactant/products into a gas sample valve setup for on-line injection.

RESULTS

In the course of this investigation several experiments related to methanol-to-hydrocarbons chemistry on H-SAPO-34 were performed. All the ^{13}C MAS NMR spectra are presented in this section and assignments of all resonances are listed in Table 1. Figure 1 shows the ^{13}C MAS NMR spectra recorded after reaction at different temperatures. The

TABLE 1

^{13}C Chemical Shift Assignments for Reactants and Products

No.	Product	Observed ^{13}C chemical shift[a]
1	CH_3OH	49.8–50.7
2	DME/Methoxy group	53–60
3	Methane[b]	−4.2, −8, −11
4	Ethane	3.27
5	Ethene	119–124
6	Propane	15.8–16.50
7	Isobutane	24.5–25
8	Butane	13.22, 25
9	Isopentane	22.68, 30.08, 32.03, 11.04
10	Pentane	13.58, 22.68, 34.3
11	2,2-Dimethylpropane	27.54, 32.03
12	3-Methylpentane	11.04, 30.08, 38, 19.53
13	Hexane	13.58, 22.44, 32.03
14	Carbondioxide	125.45
15	Aromatics (methyl substituted)	126–140, 15.04, 19.53
16	Carbonmonoxide	183–184

Note. Based on literature and multiplicity patterns obtained by proton coupling (for a few of them) (8, 43).

[a] ppm from external TMS.

[b] Three different chemical shifts correspond to different environments: −11 ppm is gas phase and −4.2 and −8 ppm are adsorbed phase.

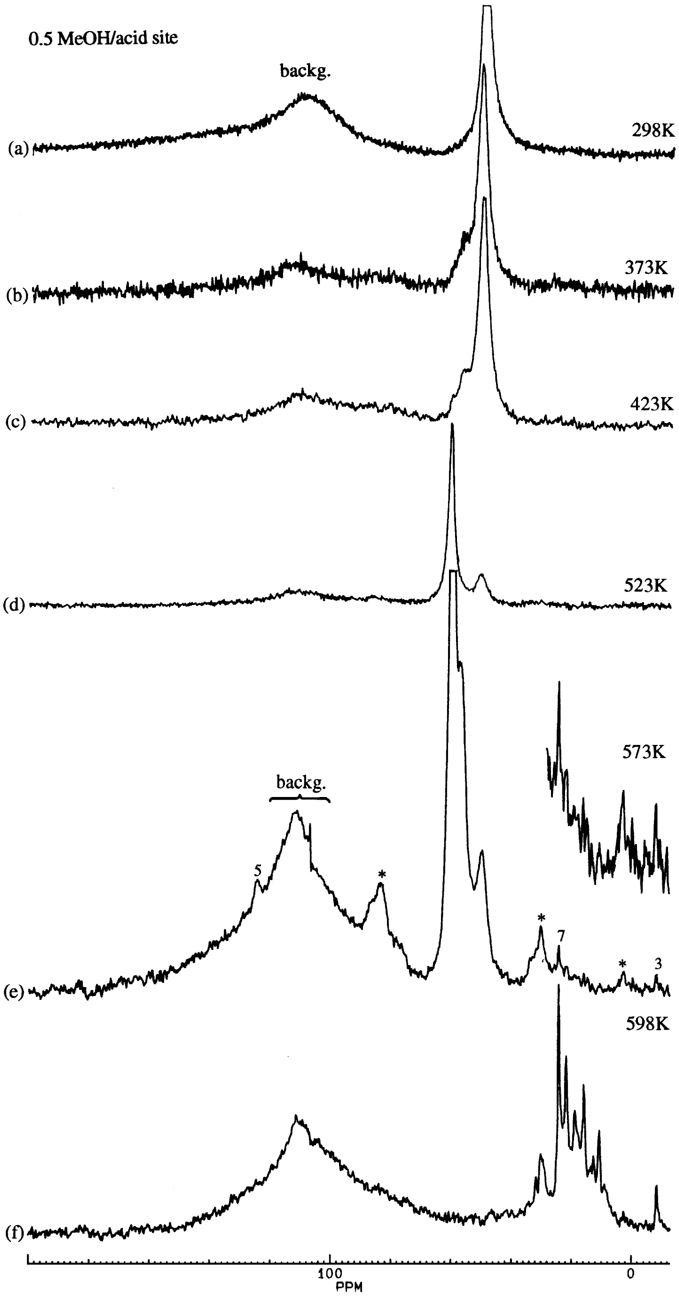

FIG. 1. ^{13}C MAS NMR spectra, with high power proton decoupling, of the sample with 0.5 : 1 (MeOH to acid site): (a) after adsorption of methanol (no thermal treatment) and after heating to (b) 373 K, (c) 423 K, (d) 523 K, (e) 573 K (the high field region is expanded to show the formation of methane and isobutane), and (f) 598 K. The asterisks denote spinning sidebands.

loading of the catalyst in this series of spectra was 0.5 : 1 MeOH molecules : acid site. After adsorption of methanol (no thermal treatment) a single broad signal at 50 ppm is observed (Fig. 1a). On heating to 373 K a spectrum consisting of two signals, one at 50 ppm and the other at 56.54 ppm assigned to both dimethyl ether (DME) and surface methoxy groups is obtained (Fig. 1b). It is worth noticing that surface methoxy groups, as reported (24), cover ranges of 53–59 ppm. Figure 1c corresponding to a temperature of 423 K clearly shows three signals, two small shoulders at 56.54 and 60 ppm on the main signal at 50 ppm ascribed to adsorbed MeOH. After exposure of the sample at 523 K (Fig. 1d) the signal at 60 ppm increases noticeably, whereas the one at 50 ppm decreases markedly. The spectrum from the sample at 573 K (Fig. 1e) exhibits methane, ethene, and isobutane, while the signals at 50 and 60 ppm are still quite intense (very low conversion in terms of hydrocarbons). On heating to 598 K a spectrum (Fig. 1f) with a multitude of narrow resonances is obtained; no signals at 50 and 60 ppm are observed. There are also no signs of any unsaturated hydrocarbons at this stage of the conversion. The relatively strong intensity of the signal at 24.5 ppm is from the contributions of butane (C_2 and C_3 positions), hexane (C_1 and C_6), and 2-methylpentane (C_1) in addition to isobutane. It seems, however, that the largest contribution is from the isobutane in the adsorbed phase. Figure 2 shows the ^{13}C MAS NMR spectra of the sample with 1 : 1 MeOH molecule : acid site at a range of temperatures. In the spectrum corresponding to 423 K (Fig. 2c) two resonances, one at 50 ppm and the other at 60 ppm, are observed. No more resonances are observed by raising the temperature to 548 K (Fig. 2d), but after heating to 573 K one resonance in the region of light aliphatics (-10 to 42 ppm) (Fig. 2e) is observed. This signal is assigned to isobutane (24.5 ppm). On heating to 598 K (Fig. 2f) the signals from other species such as isopentane and ethene appear. Further treatment to 623 K for 5 min reveals that the signals at 50 and 60 ppm are fully consumed to yield products (Fig. 2g). Of great interest in this spectrum is the appearance of aromatics, which are most clearly evidenced by the CP MAS NMR spectrum (Fig. 2h). Again, C_3 and isobutane are most abundant bearing in mind that hexane and 2-methylpentane, as mentioned above, contribute to the signal corresponding to isobutane. The sample loaded 3 : 1 methanol : acid site gave the same spectrum at temperatures 473–598 K (Figs. 3d and 3e), although this spectrum was different from the samples loaded with 0.5 : 1 and 1 : 1 methanol : acid site. It is very interesting that prolonged heating (10 min) at 598 K produces a number of C_1–C_5^+ hydrocarbons and CO (184 ppm), whereas the peaks at 50 and 60 ppm still exist (Fig. 3f). The spectrum at 623 K (10 min) reveals full conversion while CO, CO_2, and aromatics start emerging (Fig. 3h). The peaks from methanol and both DME and methoxy groups are no longer observed.

In the next stage of this study (low reaction temperatures) five more samples with the same loading as those mentioned above were treated mildly to achieve low conversion. As shown in Figs. 4–6, excluding the spectra from loading 3 : 1, the rest show hydrocarbon products in the range of C_1–C_5.

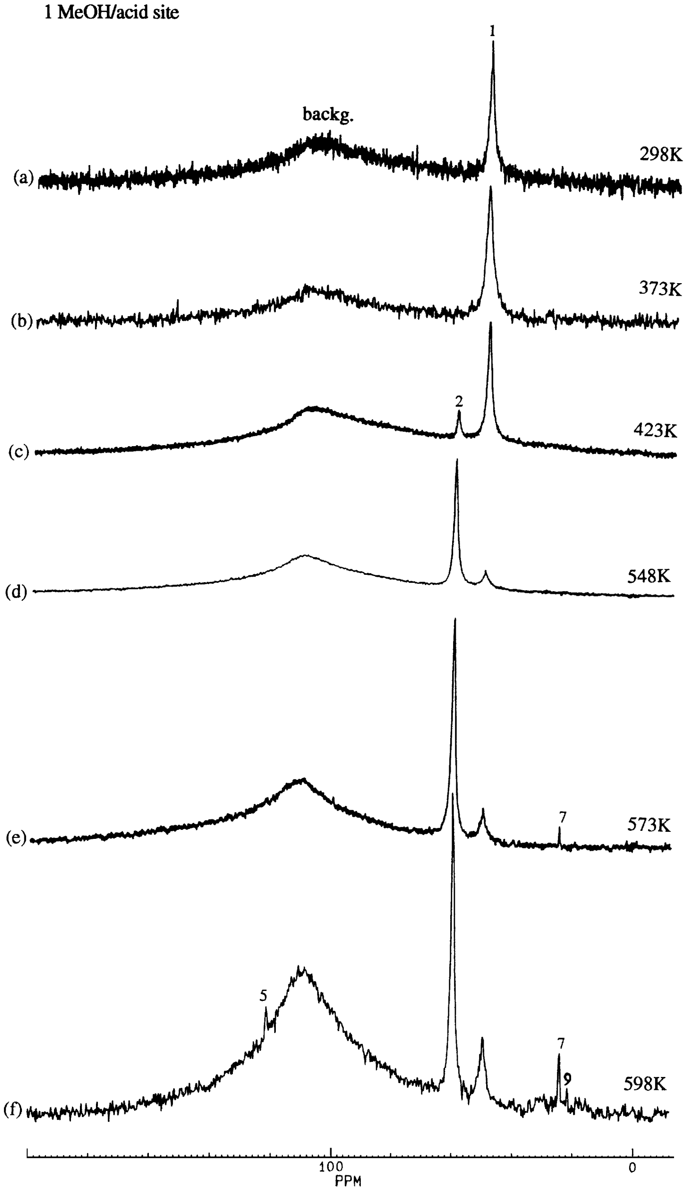

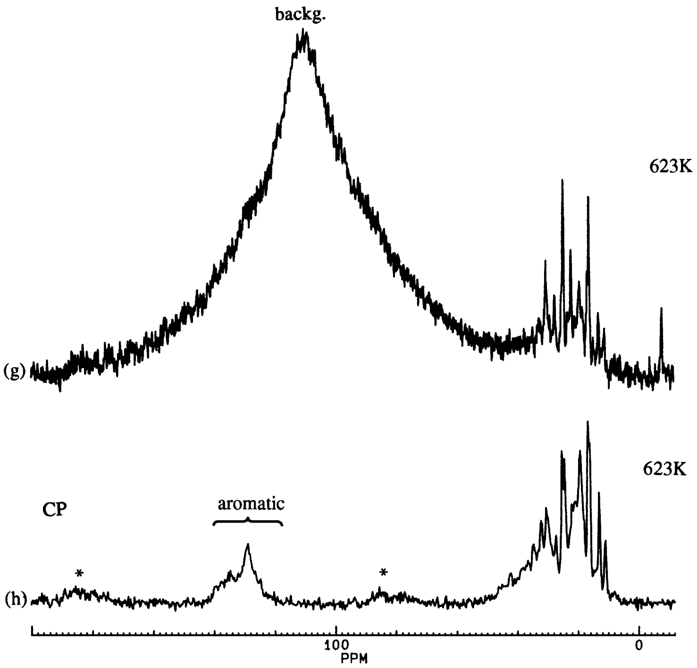

FIG. 2. ^{13}C MAS NMR spectra, with high power decoupling, of the sample with 1 : 1 methanol : acid site: (a) at room temperature (no thermal treatment) and after heating to (b) 373 K, (c) 423 K, (d) 548 K, (e) 573 K, (f) 598 K, and (g) 623 K for 5 min. (h) ^{13}C CP MAS NMR spectrum of the sample heated to 623 K. The asterisks denote spinning sidebands.

To ascertain the exact nature of the species giving rise to the 53–60 ppm resonance the following experiment was performed. A sample with methanol to Brønsted acid site 1 : 1 loading was heated at 473 K for 15 min. Any physisorbed species were then pumped off for ca. 1 h at the same temperature under high vacuum. The sample was then sealed for NMR measurements. The CP MAS spectrum (Fig. 7a) of the sample revealed a signal centered at 56.9 ppm with three small shoulders, one at low and the two others at high chemical shifts. A static ^{13}C NMR experiment of the same sample was performed in order to measure the chemical shift anisotropy of the surface species. The spectrum corresponding to this experiment (Fig. 7b) shows that the main signal at 56.9 ppm (Fig. 7a) has a powder pattern shape with an asymmetric chemical shift tensor with principal components $\delta_{11} = 91.8$, $\delta_{22} = 67.7$, and $\delta_{33} = 11.4$ ppm determined experimentally (42). Line simulation (not shown) for the spectrum in Fig. 7b gives approximately the same values for these components.

Figure 7c illustrates the ^{1}H NMR spectrum of a premethylated H-SAPO-34, showing a signal at a chemical shift of 3.96 ppm; this resonance is assigned to methyl protons. No signal was observed in the region of 9–10 ppm which might be assigned to methoxonium ion protons (44, 45). A further sample was prepared by treating H-SAPO-34 with CD_3OH at the same reaction condition as that which was utilized for the methylated sample mentioned above. ^{2}H wide-line NMR of the sample was recorded showing that there is a single Pake doublet with a splitting of ca. 36,250 Hz (Fig. 7d).

In order to show what influence ethene can have on the methanol conversion reaction we performed several NMR (batch system) and GC (flow reactor system) experiments. The spectrum (Fig. 8b) recorded from a coadsorbed sample of ^{13}C-enriched methanol and non enriched ethane heated at 523 K for 5 min clearly shows hydrocarbon product (mainly iC_5 and iC_4) in contrast with Fig. 8a where methanol was reacted alone. A marked increase in reactivity is observed (Figs. 8c and 8d) when they are allowed to react at 573 K for 2.5 and 2 min, respectively. The effect of ethene on the conversion can also be observed by adsorption of

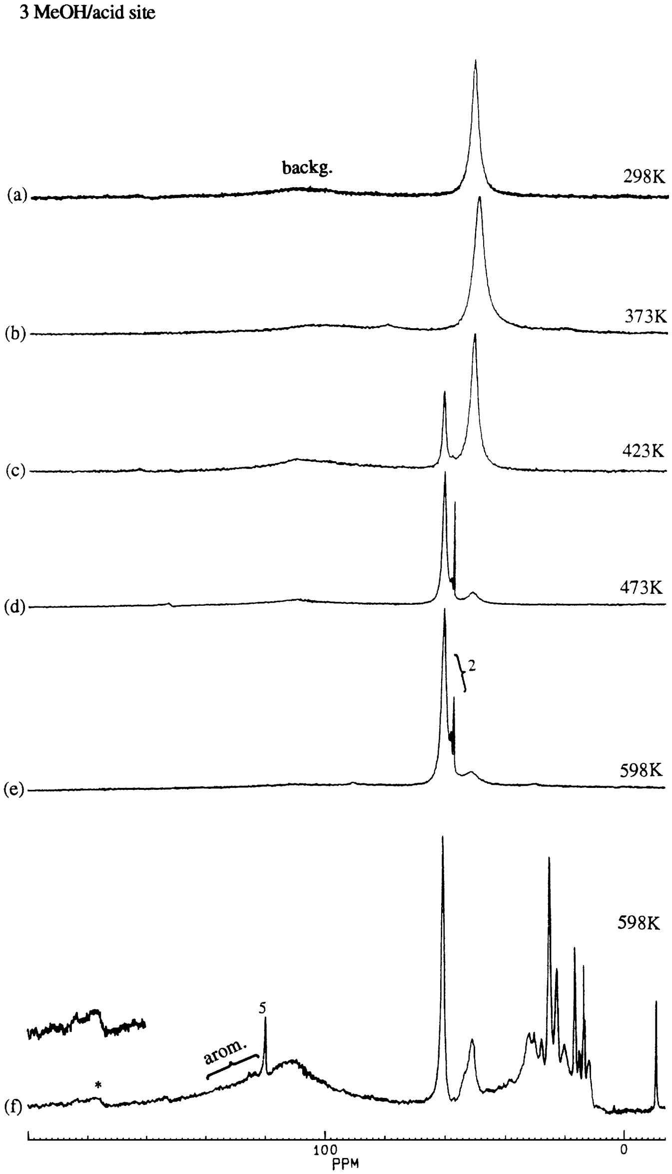

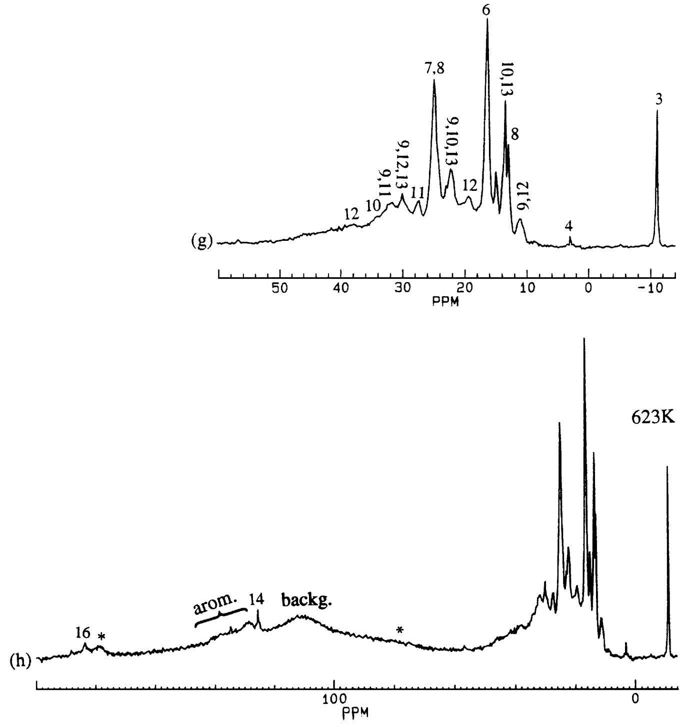

FIG. 3. ^{13}C MAS NMR spectra, with high power decoupling, of the sample with 3 : 1 (methanol to acid site): (a) after adsorption of methanol (298 K) and after heating to (b) 373 K, (c) 423 K, (d) 473 K, (e) 598 K (5 min), (f) 598 K for 10 min (the downfield region shows a weak signal at 184 ppm assigned to CO) and (h) 623 K for 10 min (the highlighted region (g) shows the component numbers as elucidated in Table 1). The asterisks denote spinning sidebands.

nonenriched ethene onto the pre-^{13}C-enriched methylated SAPO-34 when it is compared to ethene over the bare catalyst (H-SAPO-34). Their corresponding ^{13}C CP MAS NMR spectra are shown in Figs. 9a and 9b. Again a marked increase in reactivity is observed in the presence of ethene.

Reactivity of ethene over premethylated SAPO-34 was compared with that over H-SAPO-34 using a flow reactor system. To do this, methanol was first passed (WHSV = 4 h^{-1}) over the catalyst at 533 K for 1 h in order to prepare methylated SAPO-34. The carrier gas (Ar) was allowed to continue over the catalyst for one more hour at the same temperature to remove any physisorbed species. The temperature was then increased to 673 K rapidly. The column outlet was checked showing negligible amount of product and following that, ethene was immediately fed into the reactor. In the next experiment ethene was reacted over the bare catalyst under the same reaction conditions. The results of these two experiments are given in both Table 2 and Fig. 10 and show that the conversion of ethene increases by a factor of ca. 8 in the presence of surface methoxy groups compared to that over the bare catalyst.

Figure 11a from the sample loaded with ethene (1.89 molecules: acid site) clearly shows two signals assigned to ethene in both gas and adsorbed phases. No more signals appear from its CP MAS spectrum (Fig. 11b). Table 3 lists the various products at temperature of 623 K in the flow reaction system measured by a gas chromatography; ethene and methanol were separately used as reactants. A comparison between two product distributions yielded in these experiments is depicted in Fig. 12. Finally, Fig. 13 recorded from a sample after reacting in the flow system with nonenriched (^{13}C) methanol (WHSV = 6 h^{-1}) for 5 min time on stream demonstrates three relatively strong signals assigned to isobutane (24.5 ppm), C_5^+ (22 ppm), and aromatic side chains (19.16 ppm). The broad signal in the aromatic region is probably due to carbon atoms in species such as methyl-substituted polyaromatics within a coke deposit (46–48).

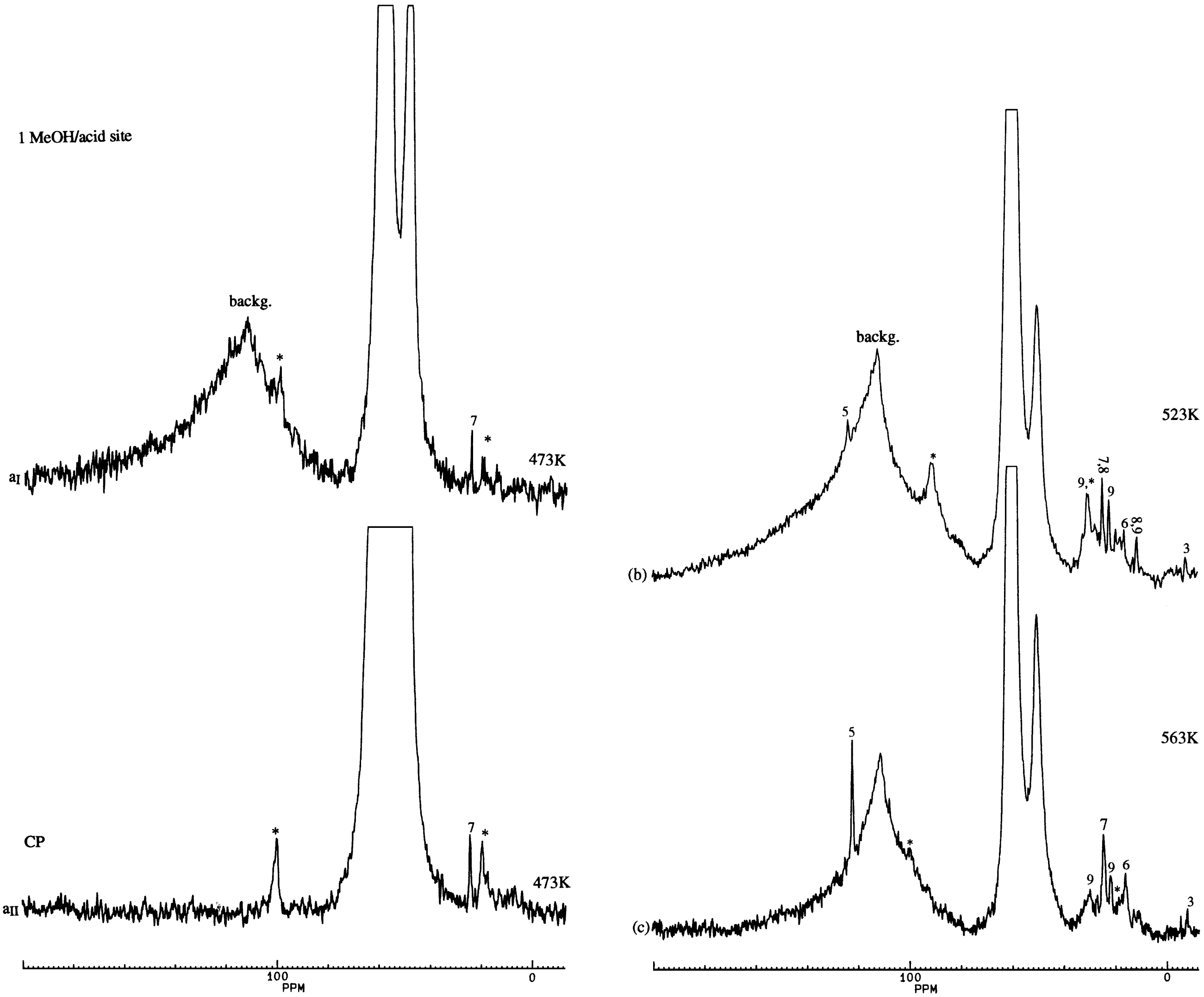

FIG. 4. ^{13}C MAS NMR spectra of three samples with 1 : 1 methanol : acid site obtained at room temperature after heating to 473 K (a_I and a_{II}) (a_{II} was recorded using ^{13}C CP MAS), 523 K (b), and 563 K (c) for 180, 30 and 10 min, respectively. The asterisks denote spinning sidebands.

DISCUSSION

There are two approaches which have been utilized in the mechanistic studies of methanol-to-hydrocarbons conversion over acidic microporous catalysts. The first approach is to study the reaction at very low conversion and high temperature ranges, 573–743 K. The second is a novel approach (performing the reaction at low temperatures < 573 K) which has received considerable attention in recent years (5, 19, 20) for gaining a better understanding of the mechanism of the formation of primary products which are involved in the first C–C bond formation.

High Temperature Experiment (Short Heating Time)

In ^{13}C MAS NMR experiments conversion can be well investigated using enriched methanol (99% ^{13}C). The primary products observed at these conditions can indeed give very indicative information concerning the mechanism of the conversion reaction. In the experiment with 0.5 : 1 methanol molecules : acid site stoichiometry the dehydration reaction (Fig. 1) commences at 373 K whereas at loadings of 3 : 1 and 1 : 1 methanol : acid site the dehydration begins at 423 K (Figs. 2c and 3c).

It is not surprising that the amount of reactant in the pores of the catalyst (loading) affects the onset of reaction. In the case of low loading (0.5 : 1 methanol : acid site) the pores are not full and dehydration proceeds freely, whereas with a loading of 1 : 1 and 3 : 1 (methanol to acid site) it is clear that the rate of the dehydration process is limited since reactant molecules themselves sterically inhibit each other toward dehydration or overcrowding of the active sites makes the catalyst less active. The spectral differences with signals for dimethylether or surface methoxy groups, at this stage of the reaction, could be the result of the difference in

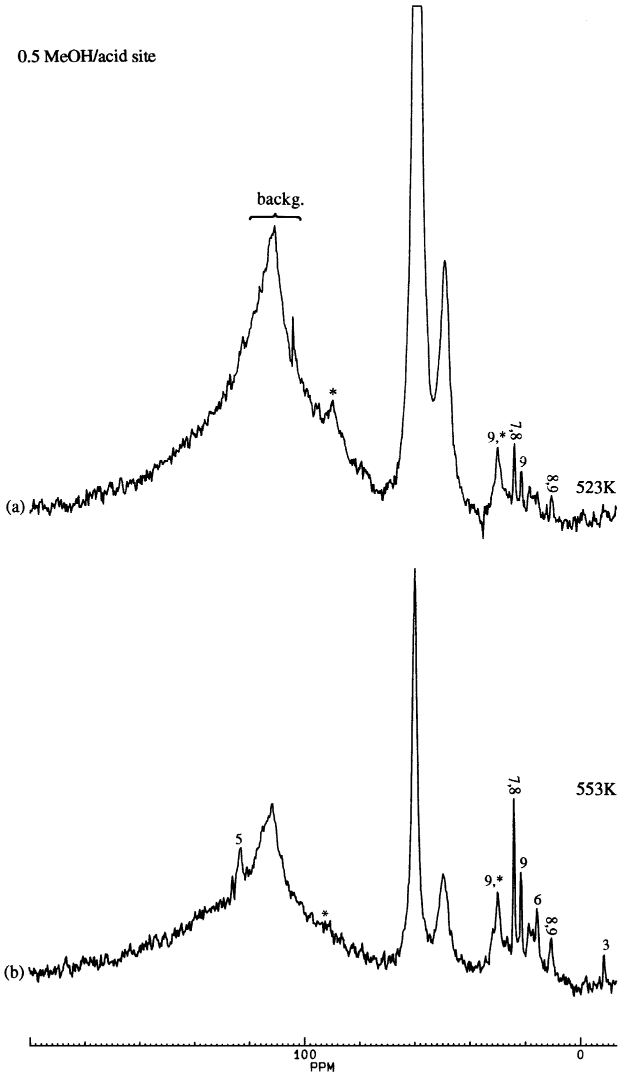

FIG. 5. ^{13}C MAS NMR spectra of the sample with 0.5 : 1 methanol to acid site after heating to: (a) 523 K for 30 min, and (b) 553 K for 10 min. Asterisks denote spinning sidebonds.

environment of the active sites of the catalyst. The next stage of the conversion reaction starts at 573 K with the formation of ethene, isobutane, and methane at a loading 0.5 : 1 (Fig. 1e) and only isobutane at a loading 1 : 1 (Fig. 2e). Once again it is observed that the loading influences the onset of hydrocarbon formation (Fig. 3e). Our observations from the sample with low loading (0.5 : 1) at 573 K (Fig. 1e) and higher loadings (1 : 1 and 3 : 1) (Figs. 2f and 3f) at 598 K (which clearly show ethene, propane, isobutane, isopentane, and a small concentration of other hydrocarbon products) imply that a type of stepwise methylation process is in progress. This mechanism will also operate at higher temperatures, e.g., the sample with 0.5 : 1; loading (reactant to acid site) at 598 K (Fig. 1f) and bogh 1 : 1 and 3 : 1 loadings at 623 K (Figs. 2g and 3h) although, at this stage of the conversion, secondary reactions will become pronounced.

Low Temperature Experiments (Long Heating Time)

Following these observations a series of experiments were carried out at temperatures 473–563 K on separate samples to find out how the conversion reaction commences at low temperatures. Interestingly, it appeared that the reaction produces the same products as those at higher temperatures. For instance, at 473 K again only isobutane is observed (Fig. $4a_{I}$) which is evidenced by its CP spectrum (Fig. $4a_{II}$), whereas at 523–563 K C_1–C_5 hydrocarbons are formed.

Mechanism

The main results which need to be accounted for when formulating a reaction mechanism are the following observations: (i) surface methoxy groups are formed at low temperatures; (ii) ethene is the smallest hydrocarbon with a C–C bond observed; (iii) under the right conditions isobutane is the first hydrocarbon observed by NMR; (iv) it appears that methane is a primary hydrocarbon product formed at the very first stage of conversion. These

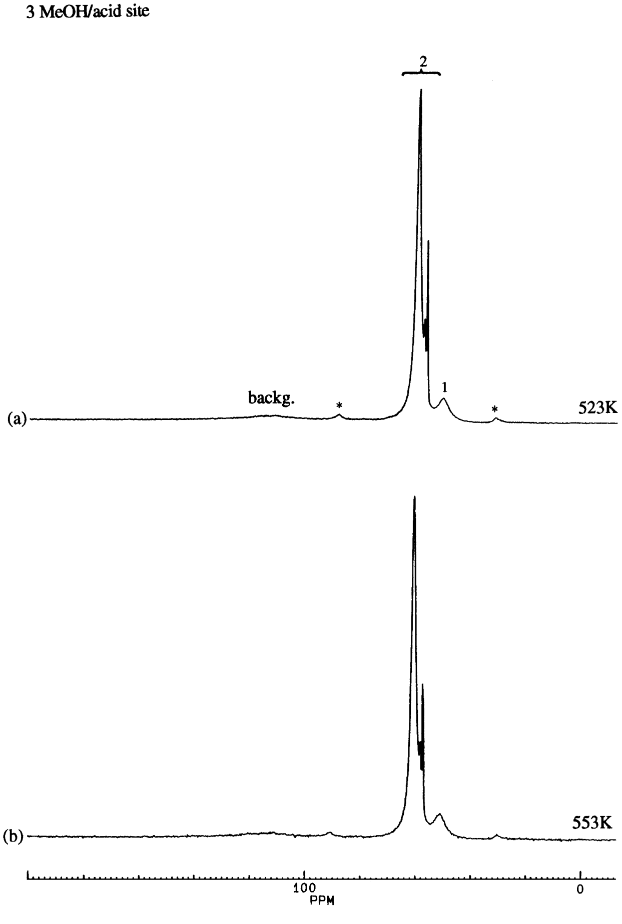

FIG. 6. ^{13}C MAS NMR spectra of the sample with 3 : 1 methanol to acid site after heating to: (a) 523 K for 30 min, and (b) 553 K for 10 min. The asterisks denote spinning sidebands.

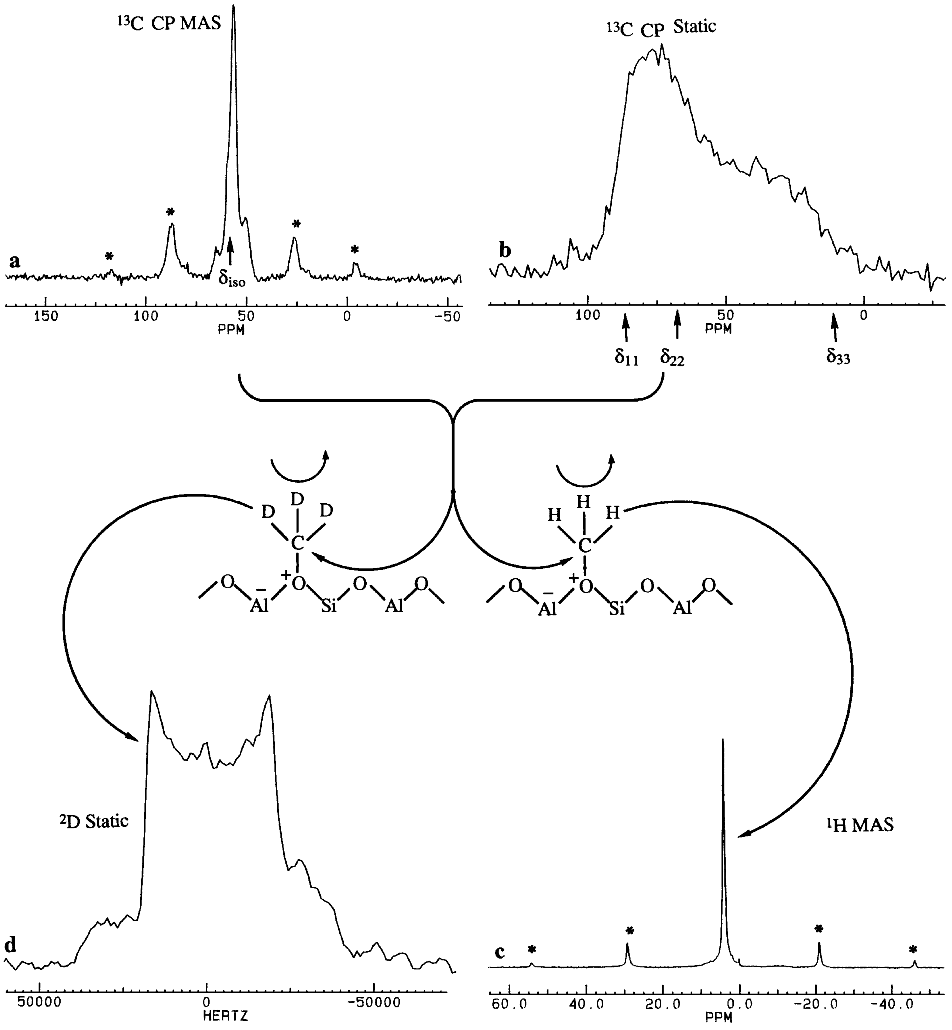

FIG. 7. (a) ^{13}C CP MAS NMR spectrum of the catalyst (1 : 1 MeOH-to-acid site loading) which reacted at 473 K (15 min) and pumped off at the same temperature (1 h), (b) ^{13}C CP static NMR of methylated H-SAPO-34 (prepared as the sample in (a), (c) ^{1}H MAS NMR of methylated H-SAPO-34 using the Hahn-echo pulse sequence, and (d) ^{2}H static NMR of D-methylated H-SAPO-34 (CD_3OH as a reactant) using quadrupolar echo sequence with composite pulses (37). The asterisks denote spinning sidebands.

observations first suggest that a common C_1 intermediate (i.e., a surface methoxy group) is involved in the formation of all hydrocarbon products. This stable surface intermediate has previously been observed by infrared spectroscopy over acidic zeolite ZSM-5 prior to the onset of hydrocarbon formation (12, 13). It has also been reported that the ^{13}C NMR signal corresponding to the surface methoxy species formed from methyl halides appears at a chemical shift range of 53–59 ppm (24, 49). We have performed a range of NMR experiments in order to confirm that these signals correspond primarily to surface methoxy groups rather than either adsorbed dimethylether or methoxonium ion (these three species would all have an isotropic ^{13}C signal in the same region of the spectrum). To this end we first performed a static ^{13}C NMR experiment which revealed an anisotropic chemical shift (CS) tensor with principal components $\delta_{11} = 91.8$, $\delta_{22} = 67.7$, and $\delta_{33} = 11.4$ ppm. By comparison gas phase dimethylether has an axially symmetric chemical shift tensor with principal components $\delta_{11} = 88$, $\delta_{22} = 88$, and $\delta_{33} = 6$ ppm (50). Consequently, dimethylether is unlikely to yield such an anisotropic CS tensor even in the adsorbed phase. Furthermore, we have performed *ab initio* calculations on the chemical shift tensor for methoxy groups and find values in close agreement with the experimental values reported here (51).

^{2}H wideline NMR of H-SAPO-34 methylated with CD_3OH shows a single Pake doublet with a quadrupole splitting of ca. 36,250 Hz consistent with a CD_3 rotation about the threefold axis, again consistent with a surface methoxy group. By contrast, absorbed dimethylether would be expected to exhibit more complex rotation which would be closer to isotropic. Finally, in order to examine the possibility of the existence of adsorbed methoxonium ions the ^{1}H highresolution spectrum was recorded. This revealed

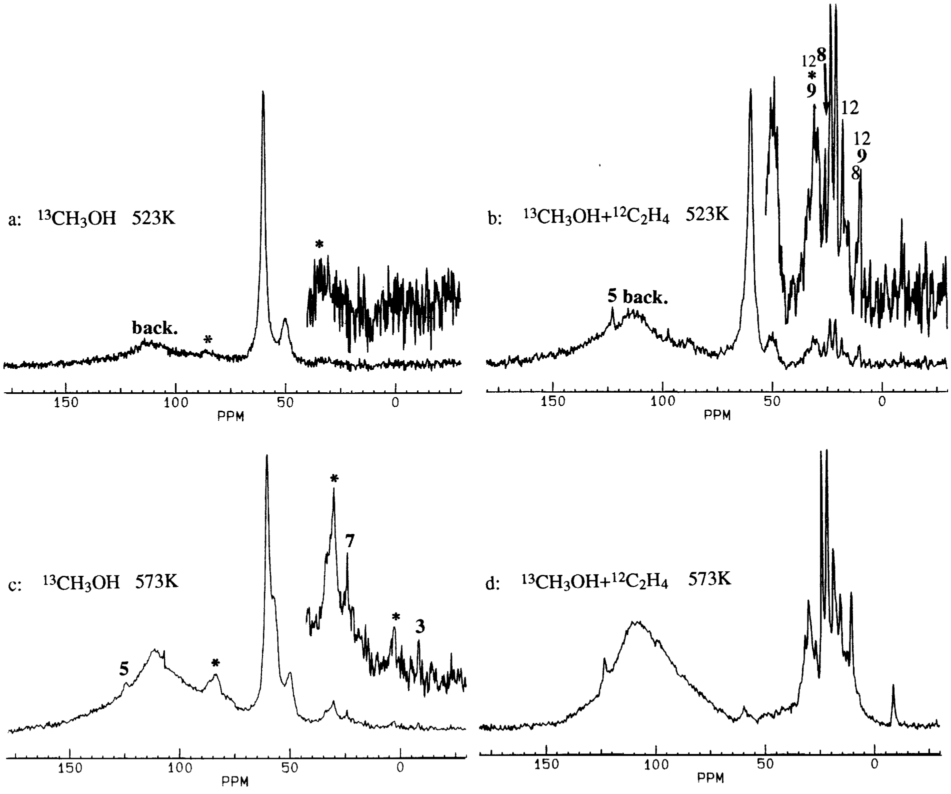

FIG. 8. ^{13}C MAS NMR obtained (a) and (c) after the conversion of ^{13}C-enriched methanol (0.5 : 1 reactant molecules per acid site) at 523 K (5 min) and 573 K (2.5 min), respectively; (b) and (d) after the conversion of $^{13}CH_3OH$ (0.5 : 1) + $^{12}C_2H_4$ (0.5 : 1) at 523 K (5 min) and 573 K (2 min), respectively. The asterisks denote spinning sidebands.

only a resonance in the region of 3.96 ppm consistent with $-CH_3$ group protons. No resonance was observed at ca. 10 ppm consistent with the hydroxyl protons of $CH_3O^+H_2$ (44, 45). Consequently, we are confident that the ^{13}C resonance at 56.9 ppm is due to surface methoxy groups. The nonaxially symmetric CS tensor mentioned above of the surface methoxy group is consistent with a configuration previously suggested from theoretical considerations whereby one methyl C–H bond is slightly elongated and points toward a neighboring framework oxygen (52). Recently it has been reported (53) that there is an apparent consensus on surface methoxy groups as the initial step in the reaction sequence of methanol over H-ZSM-5 with this species forming via the interaction of a Brønsted

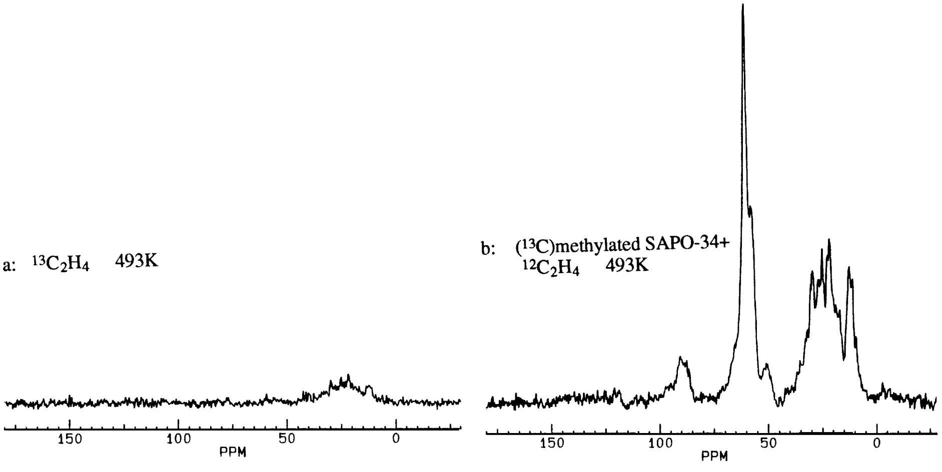

FIG. 9. ^{13}C CP MAS NMR obtained (a) after the reaction of $^{12}C_2H_4$ over H-SAPO-34 (1 : 1) at 493 K (3 min) and (b) after the reaction of $^{12}C_2H_4$ over pre-^{13}C-methylated H-SAPO-34 (1 : 1) at the same condition (temperature and heating time). Both spectra were plotted in an absolute mode.

TABLE 2

Production Distributions Obtained from the Flow Reactor System at 673 K

Experiment No.	Reactant/Catalyst	WHSV (h^{-1})	TOS^a (min)	Product (wt%) (temperature 673 K)						
				C_1	C_2	C_3	C_4	C_5^+	DME	MeOH
1	C_2H_4/H-SAPO-34	0.7	2	0.0078	98.3068	1.1442	0.2755	0.2657	—	—
2	C_2H_4/methylated SAPO-34	0.7	2	0.068	87.0482	8.5518	2.0216	2.3104	—	—

^{a} TOS = time on stream.

acid site with MeOH/DME. Our results concur with this hypothesis.

We consider three possible routes for the formation of C_2–C_4 (>C_4) products via a surface methoxy intermediate. The crucial step of all routes is the formation of ethene as a primary hydrocarbon. In accord with theoretical studies (52) which indicate that the alkyl group itself is noticeably inclined toward neighboring oxygen, polarization of the methyl C–H bond via interaction of its proton with an adjacent bridging oxygen is more likely. This has been used by Kazansky and Senchenya (52) to explain the formation of the first C–C bond via a concerted reaction of the surface methoxy group with a methanol molecule that is closely affiliated, through hydrogen bonding, with the C–H bond proton:

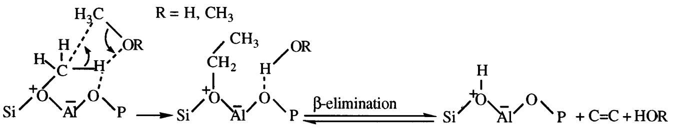

[1]

Ethane formed form this reaction can easily be methylated by reaction with surface methoxy species via the intermediacy of an alkoxy group to yield propene (route 1). Further reaction can occur with the methoxy groups to form C_4, C_5, and so on, in a process analogous to the formation of propene.

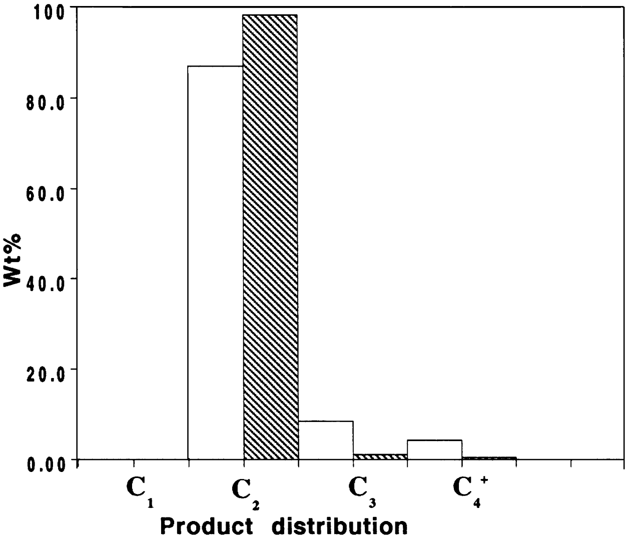

FIG. 10. Product distribution of (▨) C_2H_4 reaction over H-SAPO-34 and (□) C_2H_4 reaction over premethylated H-SAPO-34 at 673 K.

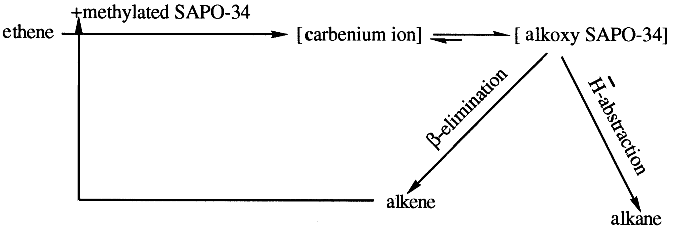

[2]

Route 1$^{(31, 54)}$

This route accompanies secondary processes at high temperature (623 K) to form light hydrocarbons (mainly C_2 and C_3) and aromatics. Dahl and Kolboe (6, 7) in a recent paper discuss the role of methylation processes in the conversion of methanol over H-SAPO-34. They conclude, based upon isotopic tracer studies, that methylation of ethene is very slow process compared to the conversion of methanol to hydrocarbons. In this work, however, we have shown that the addition of ethene, either to methanol feed or to a premethylated SAPO-34

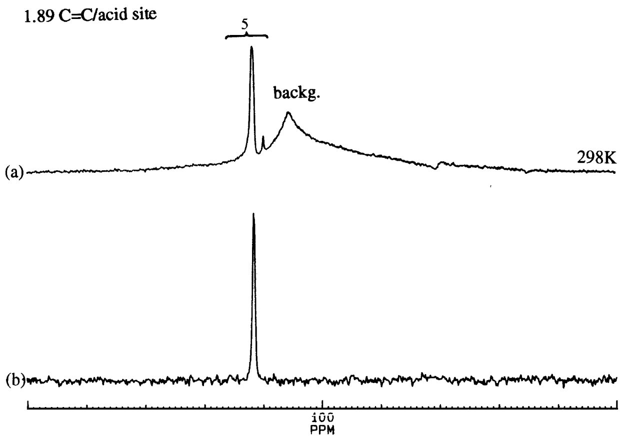

FIG. 11. (a) ^{13}C and (b) CP MAS NMR spectra of the sample loaded with ethene (1.89 molecules/acid site) at room temperature (no thermal treatment).

TABLE 3

Results of the Conversion C_2H_4 and Methanol Separately over H-SAPO-34 at 623 K

Experiment No.	Reactant	WHSV (h^{-1})	TOS (min)	Product (wt%)						
				C_1	C_2	C_3	C_4	C_5^+	DME	MeOH
1	C=C	10.48	5	0.002	95.50	2.35	1.048	1.10		
			30[a]	+	97.56	1.434	0.503	0.502		
2	MeOH	6	15	0.75	22.88	38.79	13.40	14.80	4.81	4.57

[a] Cumulative time on stream.

surface, results in enhanced hydrocarbon formation with incorporation of ethene into the products. Consequently, we believe that methylation is still an important process. At the long reaction times discussed by Dahl and Kolboe, diffusion considerations must also be taken into account. Ethene supplied as a reactant (either as neat ethene or as ethenol) will not necessarily have access to the active sites in a SAPO-34 catalyst already filled with hydrocarbon molecules. Our results reflect reaction conditions quite different from those reported previously and shed light on the system in the absence of diffusion limitations.

Route 2 involves the methylation of surface ethoxy groups by the clustering of methanol molecules around an adjacent active site via a concerted interaction to form a surface isopropoxy group (route 2)[1]. Subsequently this surface species could react either via β-elimination/hydride-abstraction to give propene/propane or by reaction with another methanol molecule in a similar faschion to yield a surface *tert*-butoxy group. This surface species must then follow route 1 to form hydrocabons larger than C_4 or finally react via β-elimination/hydride abstraction to give isobutene/isobutane (route 2):

$$\text{methylated SAPO-34} + \text{methanol} \xrightarrow{\text{via alkoxy}} \text{alkene/alkane} \quad [3]$$

Route 2$^{(52,\,15)}$

Route 3 involves the oligomerization of ethene over the active site of the catalyst:

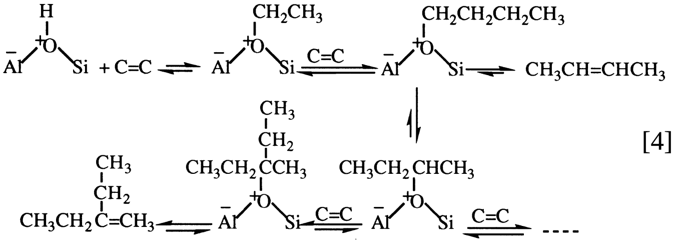

[4]

Route 3

This route has been proposed by Datema *et al.* (55) using ethene alone as reactant over H-ZSM-5. However, this mechanism requires that ethene is relatively reactive. We have checked the reactivity of ethene on H-SAPO-34 in experiments with only ethene as reactant and with methanol/ethene as coreactants. The results show the following.

(I) Ethene alone over the catalyst at room temperature in the NMR static reactor is unreactive; two ^{13}C resonances are observed, which are assigned to ethene in gas and adsorbed phases (Figs. 11a and 11b). It is also clear that in the presence of methanol or DME, which are strong bases compared to ethene, the possibility for route 3 reduces by several orders of magnitude.

(II) Ethene reaction over the catalyst using a flow–reaction system at 623 K with WHSV = 10.48 h^{-1} reveals that the conversion is less than 5% by weight (Table 3 and Fig. 12). On this basis route 3 is considered less likely to be an important mechanism on H-SAPO-34.

The mechanism outlined in route 2 implies that C_2, C_3, and C_4, being primary products, should have concentrations $C_2 > C_3 > C_4$ at the very early stages of reaction (very low

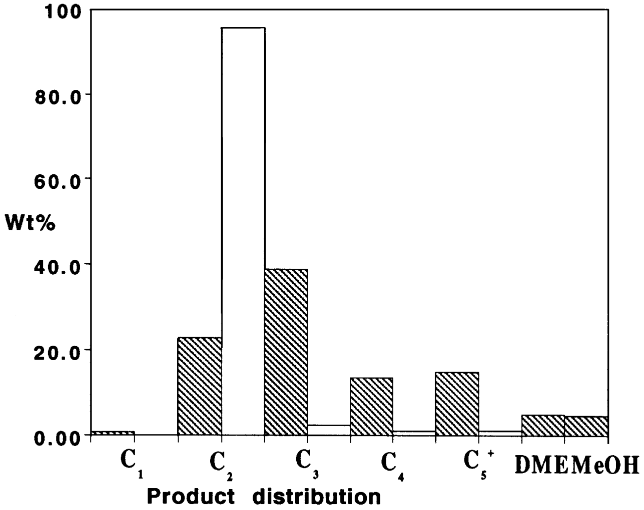

FIG. 12. Product distributions of two different reactions over H-SAPO-34 at 623 K: (□) ethene conversion and (▨) methanol conversion.

---

[1] This mechanism is aided by two neighboring active sites. With a Si/Al ratio of 0.17 for our SAPO-34 sample there is a greater than 50% probability that adjacent sites are active for catalysis.

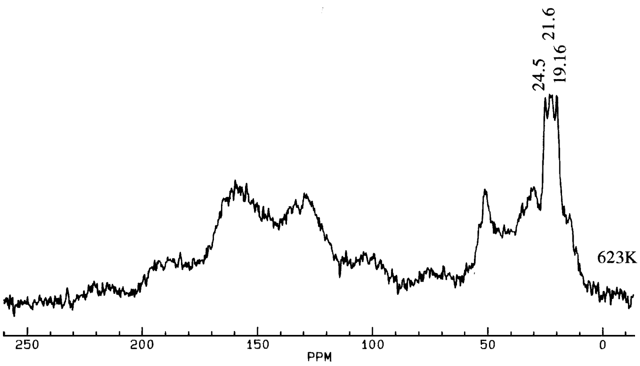

FIG. 13. ^{13}C CP MAS NMR spectrum of the sample collected after reacting with methanol at 623 K using flow reactor system (time on stream = 5 min).

conversion). This is because C_3 and C_4 products are the results of a second and third concerted interaction of a surface alkoxy species and gas phase methanol and the rate of formation of the isopropoxy and *tert*-butoxy groups is slow. Clearly, the results of our NMR experiments do not show such a concentration profile. Isobutane is always seen with the highest concentration. However, the conditions of our static microreactors must be considered. In this case we have an approximately infinite contact time and a pressure of slightly greater than 1 atm. These two factors play a significant role in shifting the equilibrium to the first stable product, i.e., isobutane (see below). Although the concentration profile of C_2, C_3, and C_4 should be different for route 1 the first stable product under static conditions should also be isobutane, Consequently, our NMR data are consistent with both route 1 and route 2.

The stability of isobutane in both route 1 and route 2 arises from the relative stability of the various alkoxy groups formed as intermediates. Methoxy groups are very stable and we have shown that these are easily observable by NMR even after heating the sample at 473 K. All other alkoxy groups, on the other hand, are very unstable and are not observed in our NMR experiments. The order of stability is as follows: ethoxy < isoproposy < *tert*-butoxy. Consequently, the concerted reactions of either route 1 or route 2 will readily form *tert*-butoxy groups under static conditions which will then react via hydride abstraction or beta elimination to form isobutane or isobutene, respectively.

The presence of ethene in our NMR spectra at the early stages of reaction will be due both to the high concentrations formed by decomposition of ethoxy groups (evidenced by the high concentration of ethene observed in flow conditions) and to the relative unreactivity of ethene. This means that even under static reactor conditions at very low conversions a small concentration of ethene will be retained. Propene, on the other hand, which is also formed in quite high concentration under flow conditions is highly reactive and will become methylated under static conditions.

Isopentane is not formed under the mildest conditions probably because the direct route via methylation of a *tert*-butoxy group is no longer available. Isobutene must desorb followed by methylation with methoxy groups and subsequent hydride abstraction. Nevertheless, isopentane is the next stable species observed by NMR after isobutane which again lends support to the idea of a methylation processes through surface methoxy groups.

The Next Stage of the Conversion Reaction

As the reaction temperature is raised (623 K) all methanol is converted to product (mainly C_4, C_3, and C_5) (Figs. 3h and 2g). By comparison with flow experiments it is expected that more C_2 and C_3 should be produced (see Table 2 and Fig. 10). A similar situation was observed previously (22) on H-SAPO-34 which was loaded with a saturation coverage of methanol. The main differences between flow conditions and the NMR experiments is due to the shape selectivity of SAPO-34 which severely restricts diffusion of molecules C_4 or greater. In the static NMR cell the long residence time results in secondary reactions such as addition, cyclization, and aromatization (Figs. 2h and 3h). However, the high abundance of C_4 and aromatics are not unique to the static system since they are also observed in a sample collected after methanol conversion in the flow system (see Fig. 13). The signal at 24.5 ppm is mainly from C_4, whereas the signals at 22 and 19.16 ppm are from C_5^+ and aromatic side chains (methyl group), respectively. These compounds, due to their large size in comparison to the catalyst aperture size, would be confined within the cages.

The formation of CO_2 and CO in the case of high loading reaction (Fig. 3h) could be from the reaction of surface methoxy species via hydride abstraction from methanol to give formaldehyde. This species could easily decompose to CO while some of the formaldehyde reacts with another molecule of methanol to yield CO_2.

Methane Formation

Based on NMR experiments performed at low temperatures, the observation of methane at very low conversion of methanol (Figs. 1e, 5b, 4b, and 4c) suggests a direct catalytic pathway for methane formation as a primary product. A mechanism with intermediacy of surface methoxy species seems to be most applicable to this formation. It has been suggested (56) that methane can form from the reaction of surface methoxy species with methanol (Reaction [5a]). This route is not entirely in agreement with our experimental findings since an equimolar amount of CO and methane should be formed. In our experiments, no CO is observed in the early stages of reaction (Figs. 1e, 5b, 4b, and 4c). However, it has also been reported (3) that coke molecules can be formed from polymerization of the formaldehyde produced via hydride donation from methanol to surface methoxy intermediate. Consequently, this may account for the absence of CO at temperatures 598–623 K (Figs. 1f, 2g) in this study (Reaction [5b]). Reaction [6] is another possible route to methane formation. In this case, the hydride source comes from large molecules deposited on the surface of the catalyst as coke, the chemical nature of which is still not fully understood. Such a scheme is possibly operative at a later stage of the conversion and methane formed via this mechanistic approach cannot be considered as a primary product:

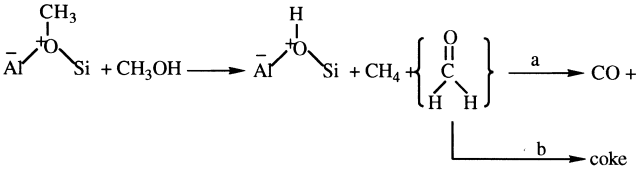

[5]

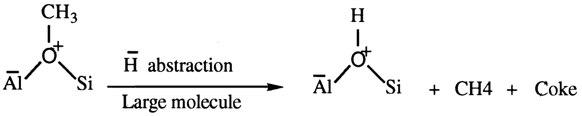

[6]

CONCLUSION

Methoxy groups formed on the surface of the acidic SAPO-34 via reaction of methanol with acid sites are considered to play a crucial key role in the formation of the first C−C bond in the methanol conversion process. Clustering of methanol around the acid environment via hydrogen bonding coupled with polarization of one of the C−H bonds of the surface methoxy groups accounts for ethene formation as the primary hydrocarbon via a concerted methylation interaction.

The presence of isobutane as the first species at very low conversion of methanol at both low and high temperatures suggests that a stepwise alkene methylation via surface methoxy groups accompanied by rearrangement of secondary butoxy to a *tert*-butoxy group is involved. It is, however, possible that a competitive sequential surface methoxy group methylation pathway (analogous to ethene formation) via a concerted interaction also exists for isobutane formation since the clustering of methanol may be a significant factor in the rapid formation of isobutane. The observation of isopentane at a very early stage of the conversion must result from methylation of isobutene via surface methoxy groups. This once again supports the mechanism of alkene methylation through surface methoxy species. Carbon monoxide and carbon dioxide which are observed at high temperature with high loading of the reactant seem to form via hydride abstraction of the surface methoxy groups from gas phase methanol to yield formaldehyde which in turn either reacts with methanol leading to CO_2, decomposes to CO, or both. The formation of methane at very low conversion and essentially at low temperature supports a mechanism with the intermediacy of surface methoxy groups. The intermediates abstract hydride ions from methanol at the very early stage of the conversion and possibly from large molecules deposited on surface of the catalyst at later stages of the conversion to yield methane as a product.

REFERENCES

1. Chang, C. D., and Silvestri, A. J., *J. Catal.* **47**, 249 (1977).
2. Bibby, D. M., Chang, C. D., Howe, R. F., and Yurchak, S., “Methane Conversion,” Elsevier, Amsterdam, 1988.
3. Hutchings, G. J., and Hunter, R., *Catal. Today* **6**, 279 (1990).
4. Hutchings, G. J., and Johnston, P., *Appl. Catal.* **67**, L5 (1990).
5. Sulikowski, B., and Klinowski, J., *Appl. Lett.* **89**, 69 (1992).
6. Dahl, I. M., and Kolboe, S., *Catal. Lett.* **20**, 329 (1993).
7. Dahl, I. M., and Kolboe, S., *J. Catal.* **149**, 458 (1994).
8. Munson, E. J., Kheir, A. A., Lazo, N. D., and Haw, J. F., *J. Phys. Chem.* **96**, 7740 (1992).
9. Munson, E. J., Kheir, A. A., and Haw, J. F., *J. Phys. Chem.* **97**, 7321 (1993).
10. Munson E. J., and Haw, J. F., *J. Am. Chem. Soc.* **113**, 6303 (1991).
11. Tabak, S. A., and Yurchak, S., *Catal. Today* **6**, 307 (1990).
12. Forester, T. R., and Howe, R. F., *J. Am. Chem. Soc.* **109**, 5076 (1987).
13. Forester, T. R., Wong, S. T., and Howe, R. F., *J. Chem. Soc. Chem. Commun.* 1611 (1986).
14. Ceckiewicz, S., *J. Chem. Faraday Trans. 1* **77**, 269 (1981).
15. Hutchings, G. J., Hunter, R., Johnston, P., and Rensburg, L. J. V., *J. Catal.* **142**, 602 (1993).
16. Hutchings, G. J., Lee, D. F., and Lynch, M., *Appl. Catal. A* **106**, 115 (1993).
17. Nováková, J., Kubelková, L., and Dolejšek, Z., *J. Mol. Catal.* **45**, 365 (1988).
18. Nováková, J., Kubelková, L., and Dolejšek, A., *J. Catal.* **108**, 208 (1987).
19. Kolboe, S., *Acta. Chem. Scand. A* **42**, 185 (1988).
20. Kolboe, S., “Proceedings, 10th International Congress on Catalysis, Budapest, 1992” (L. Guezi, F. Solymosi, and P. Tétényi, Eds.), p. 449. Akademiai Kiadó, Budapest, 1993.
21. Xu, Y., Grey, C. P., Thomas, J. M., and Cheetham, A. K., *Catal. Lett.* **4**, 251 (1990).
22. Anderson, M. W., Sulikowski, B., Barrie, P. J., and Klinowski, J., *J. Phys. Chem.* **94**, 2730 (1990).
23. Anderson, M. W., Occelli, M. L., and Klinowski, J., *J. Phys. Chem.* **96**, 388 (1992).
24. Bosáček, V., *J. Phys. Chem.* **97**, 10732 (1993).
25. Mirth, G., Lercher, J. A., Anderson, M. W., and Klinowski, J., *J. Chem. Soc. Faraday Trans. 1* **86(17)**, 3039 (1990).
26. Anderson, M. W., and Klinowski, J., *J. Am. Chem. Soc.* **112**, 10 (1990).
27. Lee, C. S., and Wu, M. M., *J. Chem. Soc. Chem. Commun.* 250 (1985).
28. van den Berg, J. P., Wolthuizen, J. P., and van Hooff, J. H. C., “Proceedings, 5th International Conference on Zeolites,” (L. V. C. Rees, Ed.), p. 649. Heyden, London, 1981.
29. Olah, G. A., *Pure Appl. Chem.* **53**, 201 (1981).
30. Olah, G. A., Prakash, G. K., Ellis, R. W., and Olah, J. A., *J. Chem. Soc. Chem. Commun.* 9 (1986).
31. Hutchings, G. J., Gottschalk, F., Hall, M. V. M., and Hunter, R., *J. Chem. Soc. Faraday Trans. 2* **83**, 571 (1987).
32. Bosáček, V., and Tvarůžková, Z., *Coll. Czech. Chem. Commun.* **36**, 551 (1971).
33. Salvador, P., and Kladnig, W. J., *Chem. Soc. Faraday Trans. 1* **73**, 1156 (1977).
34. Derouane, E. G., Gilson, J. P., and Nagy, J. B., *Zeolites 2* **42**, (1982).
35. Nováková, J., Kubelková, L., Habersberger, K., and Dolejšek, Z., *J. Chem. Soc. Faraday Trans. 1* **80**, 1457 (1984).

36. Chu, C. T.-W., and Chang, C. D., *J. Catal.* **86**, 297 (1984).
37. Hočevar, S., and Levec, J., *J. Catal.* **135**, 518 (1991).
38. Nawaz, S., Kolboe, S., Lillerud, K.-P., Stöcker, M., and Øren, H. M., *Stud. Surf. Sci. Catal.* **61**, 421 (1991).
39. Kaiser, S. W., European Patent 0 105 512 (1984).
40. Hahn, E. L., *Phys. Rev.* **80**, 580 (1950).
41. Siminovitch, D. J., Raleigh, D. P., Oleyniczak, E. T., and Griffin, R. G., *J. Chem. Phys.* **84**, 2556 (1986).
42. Herzfeld, J., and Berger, A. E., *J. Chem. Phys.* **73**, 6021 (1980).
43. Kalinowski, H.-O., Berger, S., and Braun, S., *Carbon-13 NMR Spectroscopy.* John Wiley and Sons, 1988.
44. Olah, G. A., and White, A. M., *J. Am. Chem. Soc.* **91**, 5801 (1969).
45. Anderson, M. W., Barrie, P. J., and Klinowski, J., *J. Phys. Chem.* **95**, 235 (1991).
46. Uguina, M. A., Serrano, D. P., van Grieken, R., and Venes, S., *Appl. Catal. A* **99**, 97 (1993).
47. Meinhold, R. H., and Bibby, D. M., *Zeolites* **10**, 121 (1990).
48. Weitkamp, J., and Maixner, S., *Zeolites* **7**, 6 (1987).
49. Murray, D. K., Chang, J.-W., and Haw, J. F., *J. Am. Chem. Soc.* **115**, 4732 (1993).
50. Duncan, T. M., and Hill, M., “A Compilation of Chemical Shift Anisotropies,” p. C-18. AT&T Bell Laboratories. The Farragut Press, Chicago, 1990.
51. Salehirad, F., and Anderson, M. W., in preparation.
52. Kazansky, V. B., and Senchenya, I. N., *J. Catal.* **119**, 108 (1989).
53. Hutchings, G. J., Lee, D. F., and Lynch, M., *Appl. Catal. A: General* **106**, 115 (1993).
54. Mole, T., *Stud. Surf. Sci. Catal.* **36**, 145 (1988).
55. Datema, K. P., Nowak, A. K., Houckgeest, J. van B., and Wielers, A. F. H., *Catal. Lett.* **11**, 267 (1991).
56. Wu, E. L., Kuehl, G. H., Whyte, T. E., and Venuto, P. B., *Adv. Chem. Ser. No.* **101**, 490 (1971).